Effects of barrier height inhomogeneities on the determination of the Richardson constant

K. Sarpatwari,[1,a)] S. E. Mohney,[2] and O. O. Awadelkarim[3]
[1]*Micron Technology, Boise, Idaho 83716, USA*
[2]*Department of Materials Science and Engineering, The Pennsylvania State University, University Park, Pennsylvania 16802, USA*
[3]*Department of Engineering Science and Mechanics, The Pennsylvania State University, University Park, Pennsylvania 16802, USA*

(Received 19 September 2010; accepted 23 November 2010; published online 13 January 2011)

Extraction of the Richardson constant and Schottky barrier height from the current-voltage-temperature ($I-V-T$) characteristics of Schottky barrier contacts is greatly influenced by a variety of nonideal effects. Starting with an overview of the original Richardson plot and relevant modifications of the Richardson plot, this article discusses limitations of previous analytical approaches that attempt to account for the effects of barrier height inhomogeneities on the extracted Richardson constant. A temperature-driven fundamental change in the current conduction in an inhomogeneous Schottky diode from conduction dominated by low barrier height patches to conduction dominated by high barrier height regions is identified as a likely source for the bowing of the Richardson plot, and knowledge of which regime dominates the current transport is critical for accurate determination of the Richardson constant. A simple linear relation between the effective Richardson constant and effective barrier height is described, and this recently-reported linear relation provides a consistent method for estimating the Richardson constant of inhomogeneous Schottky diodes when transport is primarily through high barrier height regions. The method is applied to $I-V-T$ characteristics of Au/Ni/n-GaN Schottky diodes measured from 320–440 K. A homogeneous Richardson constant of 29 ± 6 A cm^{-2} K^{-2} is extracted using the proposed approach and is in very good agreement with the theoretical value of 26.4 A cm^{-2} K^{-2}. © *2011 American Institute of Physics*. [doi:10.1063/1.3530868]

I. INTRODUCTION

In order to use the current-voltage ($I-V$) response to accurately obtain the metal/semiconductor (MS) Schottky barrier height, it is necessary to know the Richardson constant (A^*), and this is one of the most compelling reasons for an accurate determination of the Richardson constant.[1] The Richardson constant is extracted from the so-called Richardson plot using measured $I-V-T$ data. In practice, the extracted Richardson constant may be far from the theoretical value, and in many cases, by orders of magnitude. However, the true Richardson constant may deviate slightly from the theoretical value due to phonon scattering and quantum mechanical reflections and must therefore be determined experimentally.

Several researchers have investigated the cause for the discrepancy and proposed different explanations.[1–5] Earlier approaches (approximately mid 1980s and early 1990s) focused on the temperature and interface electric field dependence of the barrier height (as proposed by Wagner[6]), and a modified version of the Richardson plot is often used.[2,4,7,8] Recent approaches focus on incorporating the effects of barrier height inhomogeneities (BHIs) on the measured $I-V-T$ curves, including a new method[9,10] that we have proposed based on the BHI model developed by Tung.[11]

This article has been organized as follows: first, we review previous methods that are typically used to account for the deviations of the Richardson plot from the ideal case. We specifically focus on the methods that address BHIs. Next, we apply these methods to a simulated data set in order to gain insights into the applicability and limitations of these widely-used approaches. Based on the BHI framework provided by Tung, we explicitly derive the dependence of the Richardson constant on the BHI parameters. The new approach filters the effects of BHI on the extracted Richardson constant without the need for parameterized fitting or modification of the original Richardson plot. Recently, we utilized this approach to determine the Richardson constant for n-ZnO.[9,10] As further evidence for the applicability of this method, we apply the proposed approach to experimentally measured $I-V-T$ data from Au/Ni/n-GaN Schottky diodes and obtain a Richardson constant of 29 ± 6 A cm^{-2} K^{-2}. The obtained Richardson constant is in close agreement with the theoretical value of 26.4 A cm^{-2} K^{-2} for n-GaN.[12] We conclude by outlining the method as it can be applied to Richardson constant determination in other emerging semiconductor systems.

II. REVIEW OF EXISTING METHODS

In the ideal Schottky diode case, under forward bias, the carrier conduction process is limited by emission of carriers from the semiconductor over a spatially homogeneous bar-

a)Electronic mail: ksarpatwari@micron.com.

 © 2011 American Institute of Physics

rier at the MS interface into the metal. In this case, the carrier conduction, and hence the current is given by

$$I = I_{\text{sat}} \exp\left[\frac{\beta}{n}(V_a - IR_s)\right][1 - \exp(-\beta V_a)], \tag{1}$$

where

$$I_{\text{sat}} = AA^*T^2 \exp(-\beta\Phi_{\text{Beff}}). \tag{2}$$

In Eqs. (1) and (2), I is the total current, A^* is the Richardson constant, A is the diode area, β is the inverse thermal voltage (q/kT), V_a is the applied voltage, R_s is the series resistance, T is the absolute temperature, n is the ideality factor, and Φ_{Beff} is the apparent or effective Schottky barrier height.

Typically, the Richardson constant is extracted from the current-voltage-temperature $(I-V-T)$ characteristics using the Richardson plot. The saturation current, I_{sat}, is obtained from the $I-V$ data at different temperatures using

$$\ln\left(\frac{I}{1 - \exp(-\beta V_a)}\right) = \frac{\beta}{n}V_a + \ln(I_{\text{sat}}). \tag{3}$$

This equation is applicable at low currents under forward bias, where the effects of series resistance can be neglected. From the obtained I_{sat} values, the Richardson plot is constructed by plotting $\ln(I_{\text{sat}}/AT^2)$ versus $1/T$. The slope and intercept of the Richardson plot yield the effective barrier height and Richardson constant, respectively, according to

$$\ln\left(\frac{I_{\text{sat}}}{AT^2}\right) = -\frac{q\Phi_{\text{Beff}}}{k}\frac{1}{T} + \ln(A^*). \tag{4}$$

The bias and temperature dependence of the Schottky diode parameters (n and Φ_{Beff}) give rise to a slight curvature in the $\ln(I)-V$ plot. As a result of the curvature, the saturation current (I_{sat}) values used in the Richardson plot are heavily influenced by the bias range selected for curve-fitting.

A. Flat band barrier height analysis

Wagner *et al.*[6] observed a linear correlation between the ideality factor and barrier height and attributed this dependence to interface electric field dependence of the effective barrier height. A flat band barrier height (Φ_{B}^f) concept is introduced and is considered a real MS interfacial property since it is measured at zero electric field. The flat band barrier height can be expressed in terms of the ideality factor and apparent barrier height as given by

$$\Phi_{\text{B}}^f = n\Phi_{\text{Beff}} - (n-1)V_n. \tag{5}$$

In Eq. (5), V_n is the bulk potential and equals $(1/\beta)\ln(N_c/N_d)$, where N_c is the effective density of states in the conduction band and N_d is the doping density. In the case of nonideal Schottky diodes, a curvature is usually observed in the original Richardson plot. Unewisse and Storey[3] suggested a modified version of the Richardson plot using a flat band saturation current, as defined by

$$I_{\text{sat}}^f = AA^*T^2 \exp\left(-\frac{q\Phi_{\text{B}}^f}{nkT}\right). \tag{6}$$

In this case, the abscissa of the Richardson plot is modified to $1/nT$ instead of $1/T$ according to

$$\ln\left(\frac{I_{\text{sat}}^f}{AT^2}\right) = -\left(\frac{q\Phi_{\text{B}}^f}{k}\right)\frac{1}{nT} + \ln(A^*). \tag{7}$$

We label the original Richardson plot based approach [Eq. (4)] as M_1 and the flat band barrier height based approach [Eq. (7)] as M_2 for the ease of subsequent discussion.

In recent years, the inhomogeneous Schottky barrier concept has been applied to explain a wide range of observed $I-V$ characteristics. A brief overview of the inhomogeneous Schottky barrier models is presented next, in the context of their application toward modifying the Richardson plot. For the case of barrier inhomogeneities that vary on the length scale of the depletion region width, two theories are widely employed. Werner and Güttler propose an interacting Gaussian distribution of barrier heights to account for the presence of spatial inhomogeneities.[2] A central feature of this model is the assumption that the ideality factor is independent of the applied forward bias. We have not explored this approach further in this manuscript since data for Schottky barriers to n-ZnO (Refs. 9 and 10) and n-GaN that we have measured do not satisfy this constraint. On the other hand, the inhomogeneous Schottky barrier model proposed by Tung relies on a patchwork of low barrier (LB) regions embedded within a homogeneous high barrier (HB) region.[11] Tung's model accounts for bias dependence of the ideality factor, and in this article, we focus on the impact of BHIs on the Richardson plot using the framework of Tung's model.

B. Tung's model

Non-ideal behavior in the $I-V$ characteristics of a MS interface can be broadly categorized into double diode behavior and a slight curvature in the semi-log $I-V$ plot. Diodes exhibiting double diode behavior are characterized by anomalous high current at low forward bias values and are modeled as LB patches within a uniform HB region (Φ_{BH}). The LB regions are characterized by the local barrier height (Φ_{BL}) and the size of the patch (R_0). Depending on the interfacial barrier height difference between low and HB regions ($\Delta = \Phi_{BH} - \Phi_{BL}$) and the patch size, the HB region can affect the potential within the LB region. Under such conditions, the LB region may be "pinched off" by the HB region. The pinch-off phenomenon gives rise to a saddle point potential within the LB region, and the saddle point potential governs the carrier transport across the LB region. The saddle point potential is both bias and temperature dependent and can account for the observed voltage dependent Schottky diode parameters for the LB region. Tung proposed a reduced patch parameter, γ, to couple the effect of Δ and R_0 [as defined by Eq. (8)].[11] According to Tung, the double diode behavior can be modeled using a dilute density (C_1) of patches characterized by very similar γ values, where

$$\gamma = 3\left(\frac{\Delta R_0^2}{4}\right)^{1/3}. \tag{8}$$

Many Schottky diodes do not exhibit double diode behavior but they do show a slight curvature in the semilog $I-V$ plot. Tung suggests a semi-Gaussian distribution of the reduced patch parameter (γ) to account for the slight curvature in the semilog $I-V$ plot. The distribution is characterized by a peak value at $\gamma_0=0$, spread σ, and total density of patches C_1.

Consistent with Tung's model, some authors have attempted to account for the effects of BHI by using an effective area rather than the overall contact area.[7] In an inhomogeneous Schottky diode, at low temperatures, the current preferentially flows through the LB regions. In this regime, the total area contributing to the current conduction is a small fraction of the geometric area of the Schottky contact. $I-V-T$ data are fitted using the analytic expressions provided by Tung to obtain the LB patch density and σ parameters. At a given bias and temperature, the effective area of the LB patches can be estimated using

$$f=\frac{8C_1\pi\sigma^2}{9\beta_1}, \tag{9}$$

where

$$\beta_1=\left(\frac{V_{bb}}{\eta}\right)^{1/3}. \tag{10}$$

In Eq. (10), V_{bb} is the band bending at the measured bias and η is the doping density dependent parameter and equals ϵ_s/qN_d. ϵ_s is the dielectric constant of the semiconductor. The Richardson plot is then modified, using this effective area term, to

$$\ln\left(\frac{I_{\text{sat}}}{fT^2}\right)=\ln(AA^*)-\frac{q\Phi_{\text{B0}}}{kT}. \tag{11}$$

We label this method M_3 for further discussion. However, it should be noted that the effective area of the LB patches is both bias and temperature dependent.

A key aspect of this analytical approach is the hypothesis that the current contribution mainly comes from the LB regions. This assumption need not hold true across the measurement temperature range, particularly at higher temperatures. The effective area contribution is estimated using the patch spread parameter (σ) and the patch density (C_1) obtained through the $I-V-T$ fitting exercise. However, the BHI parameters (C_1 and σ) cannot be uniquely determined from the $I-V-T$ characteristics since multiple sets of BHI parameter values can fit the $I-V-T$ data. Hence, the calculation of the effective area is riddled with a great degree of uncertainty.

III. EXTENDED INHOMOGENEITY ANALYSIS

From the above discussion, it is evident that there are quite a few methods that attempt to account for the deviation of the extracted Richardson constant from the expected value. In this section, we investigate the applicability and limitations of previous methods (M_1, M_2, and M_3) using a controlled $I-V-T$ data set obtained from analytical expressions by Tung for the case of a semi-Gaussian distribution with a patch parameter γ. A wide range of device characteristics can be simulated by varying the homogeneous barrier height (Φ_{B0}) and BHI parameters (C_1 and σ). Forward bias $I-V$ characteristics are obtained across a wide range of temperature values, and the simulated data are treated in a similar fashion as one would treat experimental $I-V-T$ data. Figure 1 shows the typical simulated $I-V-T$ characteristics obtained using analytical expressions provided by Tung, as simulated using MATLAB. A patch density C_1 of 10^7 cm^{-2}, σ of 10^{-4} cm$^{2/3}$ eV$^{1/3}$, and Φ_{B0} of 1.2 eV have been used in this case.

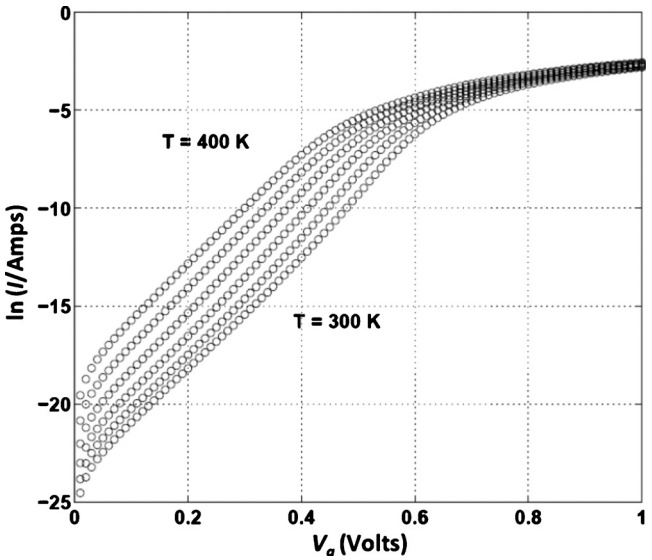

FIG. 1. $I-V-T$ characteristics simulated using Tung's equations. A homogeneous barrier height of 1.2 eV, C_1 of 10^7 cm^{-2} and σ of 10^{-4} cm$^{2/3}$ eV$^{1/3}$ have been used in this case.

A. Φ_{Beff}-n analysis

Schmitsdorf *et al.*[13] showed that the observed linear correlation between Φ_{B} and n could be explained in terms of Tung's BHI model. The linear correlation between Φ_{B} and n is reported in several MS systems and provides a simple way to account for the effects of BHI on the extracted Schottky barrier height without the need for complicated parameterized fitting of the $I-V-T$ characteristics.

However, the linear correlation observed between Φ_{B} and n is valid only for a narrow range of ideality factors, as pointed out by Schmitsdorf *et al.*[13] Figure 2 shows an Φ_{Beff}-n plot for a family of simulated devices, and each device is characterized by a different σ value. For low ideality factors $(n<1.2)$, the effective barrier height and ideality factor are linearly correlated. The linear correlation can be extrapolated to $n=n_{\text{if}}$, where n_{if} is the image force controlled ideality factor, yielding the zero-bias barrier height Φ_{B0}. Adding the zero-bias barrier height and the barrier height lowering due to the image force ($\Delta\Phi_{\text{B}}$), one can obtain the homogeneous barrier height.

The image force controlled ideality factor can be estimated using

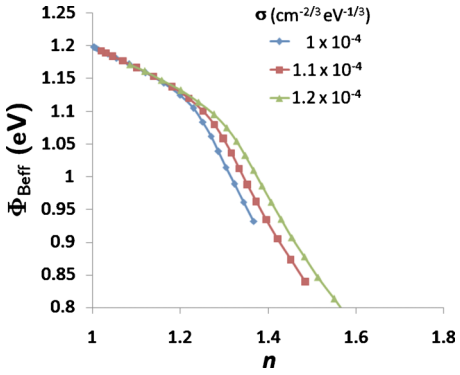

FIG. 2. (Color online) Φ_{Beff}-n plot for devices simulated with different σ values and a patch density of $C_1 = 10^7 cm^{-2}$. A homogeneous barrier height of 1.2 eV was used in the simulation.

$$n_{if} \approx 1 + \frac{1}{4}\left[\frac{q^3 N_d}{8\pi^2 \epsilon_s^3 V_{bb}^3}\right]^{1/4}, \tag{12}$$

and the barrier lowering due to image force is given by

$$\Delta\Phi_B \approx \left(\frac{q^3 N_d V_{bb}}{8\pi^2 \epsilon_s^3}\right)^{1/4}. \tag{13}$$

For moderately doped semiconductors, extrapolating to $n=1$ yields a close estimate of the homogeneous barrier height, since in this case, n_{if} is very close to 1. It should be noted that a linear correlation is observed at high ideality factor values as well, but the straight line in this region does not extrapolate to the input barrier height and can give erroneous extrapolated barrier height values. At large ideality factors, the total current is dominated by the LB regions, and although the Φ_{Beff}-n plot is linear in this regime, the extrapolated barrier height is quite different from the homogeneous barrier height. At low ideality factors, the conduction mechanism is still dominated by the homogeneous HB region, and linear extrapolation in this regime does yield the homogeneous barrier height.

B. Nonlinearity of the Richardson plot

The effect of increasing departure from ideality ($n=1$) on the Richardson plot is shown in Fig. 3. For the case of $n=1$ or low σ values, the $1/T$ and $1/nT$ plots coincide, and

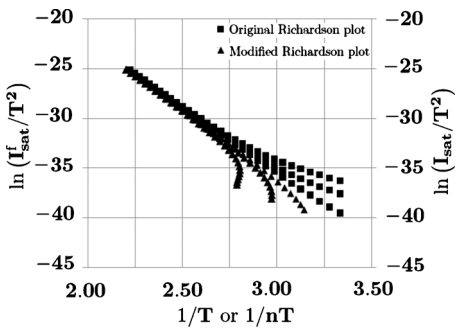

FIG. 3. Effect of σ on the Richardson and modified Richardson plot. Larger σ values correspond to greater deviation from ideality and therefore larger ideality factor values. A Richardson constant of 26 A cm^{-2} K^{-2}, homogeneous barrier height of 1.2 eV and a patch density of 1×10^7 cm^{-2} were used in the simulations. σ values in the range of $8\times10^{-5}-1\times10^{-4}$ $cm^{2/3}$ $eV^{1/3}$ were used.

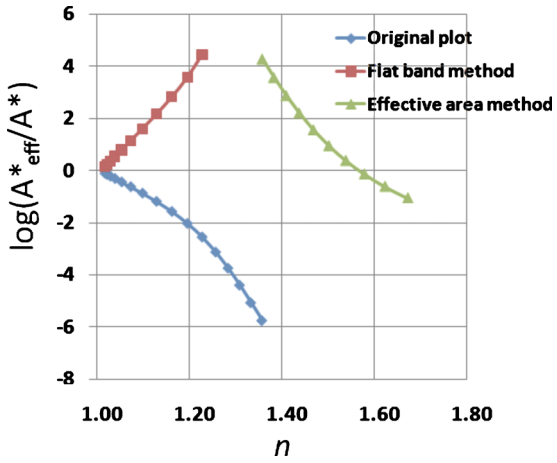

FIG. 4. (Color online) Extracted Richardson constant using the original Richardson plot (M_1), modified Richardson plot (M_2) and effective area method (M_3) as a function of extracted ideality factor. A Richardson constant of 26 A cm^{-2} K^{-2}, homogeneous barrier height of 1.2 eV and a patch density of 1×10^7 cm^{-2} were used in the simulations. σ values in the range $4\times10^{-5}-1.1\times10^{-4}$ $cm^{2/3}$ $eV^{1/3}$ were used in the simulations. In the case of extraordinarily high Richardson constant values, it has been found that the Richardson plot is no longer linear, and the method applicability is, therefore, questionable.

the obtained values of A^* and Φ_B values correlate well with the input values. For moderately high ideality factor values, the extracted A^* and Φ_B values from the original or modified Richardson plot can be quite different from the input or actual values. With increasing BHI parameter values (C_1 and σ), n tends to increase, resulting in a curvature or distortion of the Richardson plot. Curvature of the original Richardson plot has been reported widely, and in this case the modified version of the Richardson plot is often employed.[4,14–16] However, as suggested by Fig. 3, the modified Richardson plot is not always successful in rectifying the curvature observed in the original Richardson plot.

C. Application of existing methods

In order to understand the applicability of the previously reported methods, we apply these methods to analyze the $I-V-T$ characteristics from a set of simulated devices obtained by varying the BHI parameters (C_1 and σ). As mentioned earlier, we focus on three approaches: the original plot (M_1), modified plot (M_2),[3] and effective area method (M_3).[7] The original plot method is the simple original Richardson plot that does not account for any of the deviations, whereas in the modified version of the Richardson plot, the abscissa and ordinate are changed according to Eq. (7). The effective area method is a more recent approach (proposed by Roccaforte *et al.*[7]) that attempts to account for the effects of BHI on the Richardson plot by calculating the effective area for conduction using Eq. (9). In this case, the total current is assumed to be dominated entirely by the LB patches and the geometric area term (A) is scaled by an effective area term (f).

Figure 4 shows the extracted Richardson constant as compared to the input Richardson constant value as a function of σ using the three different approaches. A patch density of 1×10^7 cm^{-2}, homogeneous barrier height of 1.2 eV,

and donor density of 10^{16} cm^{-3} was used in this case. Under certain cases, extraordinarily high Richardson constant values have been extracted using this approach, and in these cases, it has been found to be that the Richardson plot is no longer linear. Forward bias $I-V$ curves simulated for the temperature range of 300–400 K were used to obtain the original and modified Richardson plots.

For low σ values (corresponding to low n), the original Richardson plot M_1 yields Richardson constant values close to the input Richardson constant. However, with increasing ideality factor values (larger n), the Richardson constant extracted using the original Richardson plot can quickly deviate from the true value. In other words, the extracted Richardson constant value is an effective value that depends on the extent of deviation the MS interface exhibits from ideality. The modified Richardson plot (M_2) also suffers from similar discrepancies and can yield reasonable Richardson constant values for low n, but with increasing n, the extracted Richardson constant can deviate significantly from the input value. The Richardson constant extracted using the effective area method M_3 can vary over orders of magnitude from the input Richardson constant value. The effective area method can yield a Richardson constant value close to the input value for large ideality factor values since the method is applicable when the contribution from LB regions dominates the total current. However, as revealed by Fig. 4, even an accurate knowledge of C_1 and σ does not ensure an accurate determination of the actual Richardson constant since the effective area is in reality both bias and temperature dependent.

IV. NEW APPROACH

Using the analytic expressions for $I-V-T$ and pertinent approximations in the HB dominated regime, we derived the effect of BHI parameters on the effective Richardson constant value (A^*_{eff}). The Richardson constant (A^*_{eff}) obtained was shown to be related to the effective barrier height (Φ_{Beff}). In the HBD regime, the homogeneous parameters (A^* and Φ_{B0}) are related to the effective parameters (A^*_{eff} and Φ_B) by

$$\ln(A^*_{eff}) = \ln(A^*) + \left(\beta - \frac{1}{\beta\beta_1^2\sigma^2}\right)(\Phi_{Beff} - \Phi_{B0}). \quad (14)$$

The detailed derivation of Eq. (14) has been outlined in an earlier publication.[9,10] Equation (14) suggests that the extracted effective barrier height and Richardson constant are correlated, and as Φ_B approaches the homogeneous barrier height, the effective Richardson constant approaches the unaffected, homogeneous value (A^*). In other words, in the HB dominated regime, with diminishing BHI, both the effective barrier height and Richardson constant values approach their true values in a correlated fashion.

Figure 5 shows a typical $\log(A^*_{eff})-\Phi_{Beff}$ constructed using the extracted Richardson constant and effective barrier height values from several simulated devices. A homogeneous barrier height of 1.2 eV and A^* of 26 A cm^{-2} K^{-2} were assumed in this case. C_1 and σ values were chosen randomly within the range $1-5\times10^7$ cm^{-2} and 0.9–1.1

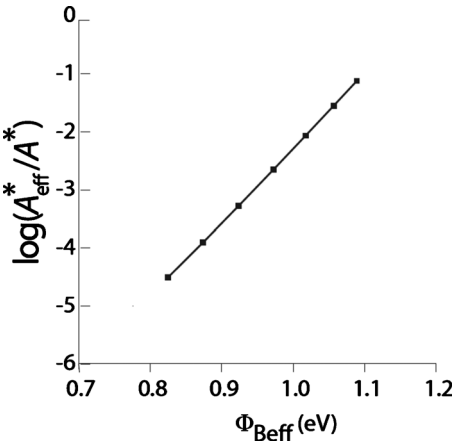

FIG. 5. Linear correlation between $\ln(A^*_{eff})$ and Φ_{Beff} extracted from the original Richardson plot for several simulated devices. An input barrier height of 1.2 eV and Richardson constant of 26 A cm^{-2} K^{-2} have been assumed in this case.

$\times10^{-4}$ $cm^{2/3}$ $eV^{1/3}$, respectively, to generate the data points on the plot. As mentioned earlier, in the HB regime, the Φ_{Beff}-n plot can be extrapolated to the homogeneous barrier height. The HB regime is indicated by the absence of bowing in the Richardson plot. The $\ln(A^*_{eff})$-Φ_{Beff} plot is constructed using the $\ln(A^*_{eff})$ and Φ_{Beff} values obtained from a set of devices using data from the HB-dominated regime. The homogeneous Richardson constant can then be extracted by extrapolating the $\ln(A^*_{eff})$-Φ_{Beff} plot to $\Phi_{Beff}=\Phi_{B0}$. The zero-bias barrier height can be obtained from the Φ_{Beff}-n plot by extrapolation to $n=n_{if}$. Extrapolating the $\ln(A^*_{eff})$-Φ_{Beff} plot to the homogeneous barrier height, a homogeneous Richardson constant value of 26.2 A cm^{-2} K^{-2} is obtained and matches the input Richardson constant.

It needs to be noted that at larger ideality factors, the Φ_{Beff}-n plot does not yield the homogeneous barrier height. Under these conditions, the Richardson plot will be nonlinear, and even if the $\ln(A^*_{eff})$-Φ_{Beff} plot is linear for this regime, the extrapolation might not yield the homogeneous Richardson constant.

V. APPLICATION TO EXPERIMENTAL *I–V–T* DATA

Au/Ni/n-GaN Schottky barrier diodes

A GaN epilayer doped with Si grown on a sapphire substrate was used for Schottky diode fabrication. Prior to the ohmic contact and Schottky metal deposition, the sample surface was cleaned using 10% HCl for 45 s. The Ohmic contact was formed by depositing Ti/Al/Ni/Au layers of 30/120/50/20 nm thickness using e-beam evaporation followed by rapid thermal annealing at 800 °C for 60 s. Circular contacts (area=10^{-3} cm^2) of Ni/Au (50/150 nm) were deposited using e-beam evaporation, and the contacts were defined using lift-off. A net donor concentration of 1×10^{17} cm^{-3} was determined from capacitance-voltage measurements of the Schottky contacts.

For the $I-V-T$ measurements, the sample was mounted on a hot stage, and the temperature was controlled and monitored using a Temptronics temperature controller, chromel-alumel thermocouple and a Keithley 2000 temperature mea-

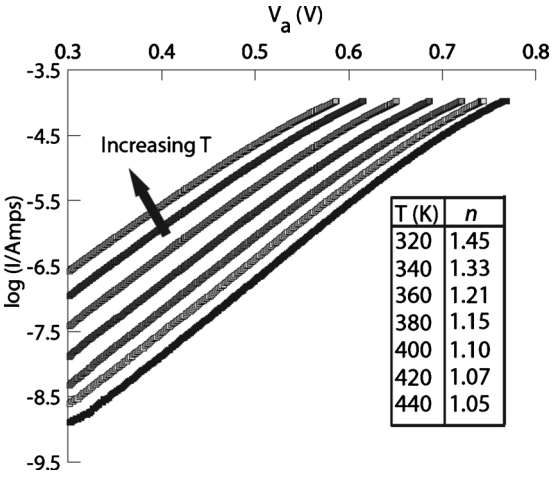

FIG. 6. Typical $I-V-T$ characteristics measured for Au/Ni/n-GaN Schottky diodes.

surement system. Electrical characterization was performed using a Keithley 4200 Semiconductor Characterization system. $I-V-T$ characteristics of the Au/Ni/n-GaN Schottky diodes were measured from 320–440 K, and a typical plot on a semi-log scale is shown in Fig. 6. The diodes exhibit an ideality factor of about 1.45 at $T=320$ K, and the ideality factor decreases to about 1.05 at $T=440$ K. The high ideality factor values obtained at lower temperatures can be attributed to the presence of BHIs. Contribution due to field emission can be neglected due the low doping density in these diodes. With increasing temperature the LB region contribution becomes less significant, and the current conduction becomes more spatially homogeneous (ideality factor close to one).

Figure 7 shows a typical Richardson plot obtained from the $I-V-T$ data of the n-GaN Schottky diodes. As evident in Fig. 7, the effect of BHI is manifested as a curvature in the original Richardson plot.

Applying Eqs. (3) and (4) to the $I-V-T$ data measured in the high temperature regime, we obtain the barrier height and Richardson constant for different diodes. Due to the presence of BHI, these values are expected to differ from the homogeneous values and are deemed as effective ones. Table I shows the extracted barrier height and Richardson constant values for different devices. The extracted Richardson constant values show a scatter over several orders of magnitude and are, also, orders of magnitude lower than the theoretical

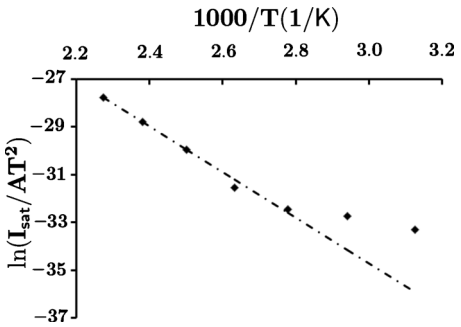

FIG. 7. Typical Richardson plot obtained for one of the Au/Ni/n-GaN Schottky diodes.

TABLE I. Extracted Richardson constant values for different GaN Schottky diodes obtained using the original Richardson plot.

Device No.	A^*_{eff} (A cm^{-2} K^{-2})	Φ_{Beff} (eV)	n (380 K)
1	1.3×10^{-2}	0.88	1.22
2	3.2×10^{-2}	0.89	1.18
3	7.1×10^{-4}	0.77	1.28
4	3.1×10^{-3}	0.82	1.25

value of 26.4 A cm^{-2} K^{-2}. Depending on the extent of BHI, the extracted Richardson constant is found to vary greatly from device to device.

Figure 8 shows the Φ_{Beff}-n plot, and extrapolating the observed linear correlation to $n_{\text{if}}=1.01$ [estimated using Eq. (12)], a zero-bias barrier height of 1.12 ± 0.01 eV is obtained. Figure 8 shows the correlation observed between the extracted barrier height and Richardson constant values on a semi-log scale. As suggested by our preceding discussion, as the barrier height increases toward the homogeneous barrier height, the extracted Richardson constant value increases from a low value toward the theoretical Richardson constant. Utilizing the zero-bias barrier height obtained from the above analysis and estimating the barrier height lowering term [from Eq. (13), Ref. 13] to be around 15 mV, a homogeneous barrier height of 1.14 eV can be obtained.

A homogeneous Richardson constant value of 29 ± 6 A cm^{-2} K^{-2} can be obtained using Fig. 8 and Φ_{BH}. The homogeneous Richardson constant is in close agreement with the theoretically expected value of 26.4 A cm^{-2} K^{-2}.[12] It is important to note that a wide range of A^* values have been reported in the literature.[17–21] The sometimes large discrepancy between experimentally observed A^* and the theoretical value is typically attributed to inferior diode quality. However, even for diodes exhibiting low ideality factors, the extracted Richardson constant can vary over orders of magnitude. The proposed approach overcomes this difficulty by filtering the effects of BHI on the extracted Richardson constant value, allowing a more accurate determination of the true Richardson constant, which can deviate from the theoretical value slightly due to quantum mechanical reflections and phonon scattering and must therefore be determined from experiments.

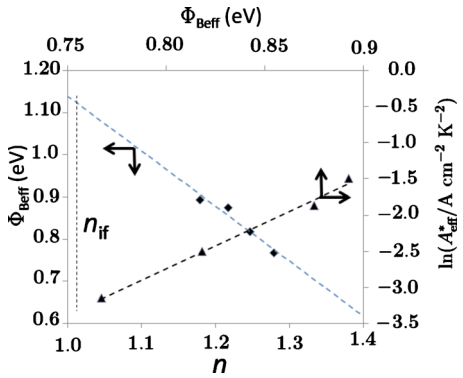

FIG. 8. (Color online) Linear correlations between Φ_{Beff}-n values and Φ_{Beff}-ln(A^*_{eff}) values.

VI. CONCLUSIONS

Previously proposed approaches to extract the Richardson constant are described. These currently employed methods can provide inaccurate results and fail to effectively filter the effects of BHI. In this article, we have elaborated upon the limitations of these approaches through evaluation of simulated data sets, and we have also provided details on a new approach we recently reported.[9,10] The new method is based on Tung's BHI model and takes advantage of a linear correlation between the extracted Richardson constant and the effective barrier height. In this paper, the method is applied to Au/Ni/n-GaN Schottky diodes as a second example of its applicability.

Based on the preceding analysis and discussion, we can provide a few simple guidelines that are useful to account for the effects of BHI on the extracted Richardson constant. One of the key points to be noted is that even in the case of moderate ideality factors ($\sim$1.1), the extracted Richardson constant can be significantly different from the actual value when determined using the original or modified Richardson plot or the effective area method. When the Richardson plot exhibits bowing, higher measurement temperatures should be used, instead of using the modified Richardson plot. In the case of MS diodes with low homogeneous barrier heights, adequately high temperatures might not be accessible since $I-V-T$ measurements are further complicated due to series resistance or interfacial reactions at high temperatures. After choosing the appropriate temperature window, the original Richardson plot can be used to extract an *effective* Richardson constant and *effective* barrier height for each of a set of devices. These values can then be used to construct the $\ln(A^*_{\text{eff}})$ versus Φ_{Beff} plot. In order to obtain the homogeneous Richardson constant, one would need the zero-bias barrier height, and this can be obtained from the Φ_{Beff}-n plot, constructed from the n values in the HBD regime along with the effective barrier heights.

Using the proposed linear correlation, along with the widely-used Φ_{Beff}-n plot, we have analyzed simulated $I-V-T$ data from the semi-Gaussian BHI model and actual Au/Ni/n-GaN Schottky diodes. Excellent correlation between the expected and extracted values has been shown for the two cases. The proposed method is particularly valuable for semiconductor systems that are still shrouded in uncertainty due in part to immature crystal growth and processing methodology. Apart from the Au/Ni/n-GaN Schottky diodes, we have applied this method successfully to the Richardson constant determination of n-type melt grown ZnO.[9]

ACKNOWLEDGMENTS

The authors are grateful to Dan Ewing for sharing the Au/Ni/n-GaN Schottky diodes and to Martin Allen, Steve Durbin, and W. Mönch for useful suggestions.

[1] M. Missous and E. H. Rhoderick, J. Appl. Phys. **69**, 7142 (1991).
[2] J. H. Werner and H. H. Güttler, J. Appl. Phys. **69**, 1522 (1991).
[3] M. H. Unewisse and J. W. V. Storey, J. Appl. Phys. **73**, 3873 (1993).
[4] S. Hardikar, M. Hudait, P. Modak, S. Krupanidhi, and N. Padha, Appl. Phys. A: Mater. Sci. Process. **68**, 49 (1999).
[5] P. G. McCafferty, A. Sellai, P. Dawson, and H. Elabd, Solid-State Electron. **39**, 583 (1996).
[6] L. F. Wagner, R. W. Young, and A. Sugerman, IEEE Electron Device Lett. **4**, 320 (1983).
[7] F. Roccaforte, F. L. Via, V. Raineri, R. Pierobon, and E. Zanoni, J. Appl. Phys. **93**, 9137 (2003).
[8] F. Iucolano, F. Roccaforte, F. Giannazzo, and V. Raineri, J. Appl. Phys. **102**, 113701 (2007).
[9] K. Sarpatwari, O. O. Awadelkarim, M. W. Allen, S. M. Durbin, and S. E. Mohney, Appl. Phys. Lett. **94**, 242110 (2009).
[10] K. Sarpatwari, O. O. Awadelkarim, M. W. Allen, S. M. Durbin, and S. E. Mohney, Appl. Phys. Lett. **95**, 059901 (2009).
[11] R. T. Tung, Phys. Rev. B **45**, 13509 (1992).
[12] M. R. H. Khan, T. Detchprohm, P. Hacke, K. Hiramatsu, and N. Sawaki, J. Phys. D: Appl. Phys. **28**, 1169 (1995).
[13] R. F. Schmitsdorf, T. U. Kampen, and W. Monch, J. Vac. Sci. Technol. B **15**, 1221 (1997).
[14] S. Acar, S. Karadeniz, N. Tugluoglu, A. B. Selcuk, and M. Kasap, Appl. Surf. Sci. **233**, 373 (2004).
[15] S. Asubay, O. Gullu, B. Abay, A. Trt, and A. Yilmaz, Semicond. Sci. Technol. **23**, 035006 (2008).
[16] A. F. Hamida, Z. Ouennoughi, A. Sellai, R. Weiss, and H. Ryssel, Semicond. Sci. Technol. **23**, 045005 (2008).
[17] P. Hacke, T. Detchprohm, K. Hiramatsu, and N. Sawaki, Appl. Phys. Lett. **63**, 2676 (1993).
[18] A. C. Schmitz, A. T. Ping, M. A. Khan, Q. Chen, J. W. Yang, and I. Adesida, Semicond. Sci. Technol. **11**, 1464 (1996).
[19] A. Ping, A. Schmitz, M. A. Khan, and I. Adesida, Electron. Lett. **32**, 68 (1996).
[20] L. Wang, M. I. Nathan, T. Lim, M. A. Khan, and Q. Chen, Appl. Phys. Lett. **68**, 1267 (1996).
[21] E. J. Miller, E. T. Yu, P. Waltereit, and J. S. Speck, Appl. Phys. Lett. **84**, 535 (2004).